3D3-3

Attenuation Characteristics of the SAR in a COST244 Phantom with Different EM Source Locations and Sizes

Shoichi Kajiwara, Atsushi Yamamoto, Koichi Ogawa, Akihiro Ozaki, and Yoshio Koyanagi

†Matsushita Electric Industrial Co., Ltd.   1006, Kadoma City, Osaka, 571-8501 Japan

E-mail: †kajiwara.shoichi@jp.panasonic.com

1. INTRODUCTION

In recent years, a number of studies have been made on the SAR (Specific Absorption Rate) caused by an antenna of mobile phones close to a head of an operator [1]-[3]. The SAR is defined by the following equation:

$$SAR = \frac{\sigma E^2}{\rho} \quad [\text{W/kg}] \qquad (1)$$

where E [V/m] is the amplitude of effective value of the electric field, σ [S/m] and ρ [kg/m^3] are the electric conductivity and the density of human tissue, respectively.

In general, an approximation of a plane wave for the electromagnetic field has been applied to E in eq. (1) in order to represent the SAR characteristics in the internal parts of the head [1], [4]. For example, attenuation characteristics of the SAR inside a phantom are determined from an empirical formula in [1]. However, the electric field radiated from the antenna is considered to be a spherical or a cylindrical wave since a mobile phone is used close adjacent to the human head.

The authors have proposed a new measurement system of the SAR that makes use of a noble algorithm that predicts the SAR from the measurement of the magnetic field distribution in the vicinity of a cellular radio in free space [5]. In this procedure, the average SAR is calculated by the 3-dimensional SAR distribution in a cubic shape that is estimated from the SAR on a phantom surface using an attenuation constant of the liquid in the phantom. Thus, an accurate evaluation of the attenuation constant is essential for this measurement system.

This paper presents a formula to provide more accurate attenuation characteristics of the SAR, which takes a spatial attenuation factor of the electromagnetic field of a spherical or a cylindrical wave into consideration. Attenuation characteristics of the SAR in a COST244 phantom that simulates the human head are evaluated with different electromagnetic source locations and sizes using the FDTD technique. From this, some physical pictures regarding the attenuation characteristics in a lossy media of the COST244 phantom are clearly understood. The analysis shows that excellent agreement between predictions using the formula and the calculated quantities is obtained.

2. CALCULATION MODEL

Figure 1 shows the calculation model used in this paper. The COST244 model [6] was used as a human phantom. This model of a head was homogeneous and had a relative permittivity ε_γ = 41.5, a conductivity = 0.95 S/m, and density ρ = 1000 kg/m^3, which are the electric constants simulating the brain tissue. A half-wavelength dipole at 900 MHz with a length of 160 mm was used as a radiation source. A continuous wave with an input power of 250 mW was radiated. The distance between the antenna and the surface of the human head model was d mm. The origin of the coordinates was set at the center of the surface of the human head model, immediately under the feeding point of the antenna. The FDTD method was used for analytical calculation purposes. The cell size in the analysis area was $\Delta x = \Delta y = \Delta z = 2.5$ mm; the absorbing boundary condition was an eight-layer PML (perfect matched layer). The value of SAR evaluated in this paper was normalized by that of $SAR(0)$, which was obtained at a depth of a half cell (1.25 mm) for the FDTD analysis.

3. ATTENUATION CHARACTERISTICS OF THE SAR

Figure 2 shows the attenuation characteristic of the SAR inside the human head model when the distance between the antenna and the model (d) was changed from 2.5 mm to 100 mm. The horizontal axis represents the distance y from the surface of the human head model, and the vertical axis represents the value of SAR normalized by $SAR(0)$ at the surface. The solid line shows the attenuation characteristic calculated by the attenuation constant of the plane wave [4]. Each bullet shows the result of FDTD analysis when the distance d is changed.

As seen in Fig. 2, the results when $d \geq 50$ mm (shown as ▲ and ×) agree well with those of the plane wave shown by the solid line. On the other hand, when $d < 50$ mm shown by □, ◊, ●, and ∆ in Fig. 2, the attenuation is steeper than that of the plane wave. This reveals that the distance between the antenna and the surface of the head model

greatly influences the attenuation characteristics of the SAR in the medium. From this, the attenuation characteristics of the SAR cannot be expressed as that caused by a plane wave incidence when the antenna is located close to the head.

4. CONSIDERATION OF THE SPATIAL SPREAD OF ENERGY

Let the attenuation constant of the electric field in the media be α [Np/m] [4] and the SAR value on the surface of media be $SAR(0)$, then since $SAR \propto E^2$ from eq. (1), the value of the SAR in the direction of y is generally given by:

$$SAR(y) = SAR(0) \cdot \exp(-2\alpha y) \qquad (2).$$

Here, the energy of the electromagnetic wave propagating along the y axis is considered to be attenuated proportionally to $(1/y)^n$ in accordance with the law of energy conservation. n is determined to be 0, 1, and 2 for a plane wave, cylindrical wave, and spherical wave, respectively.

Consequently, a formula to represent the attenuation characteristics of the SAR is proposed by multiplying eq. (2) by a term expressing the spatial spread of energy.

$$SAR(y) = SAR(0) \cdot \frac{\exp(-2\alpha y)}{(y/d+1)^n} \qquad (3)$$

In eq. (3), the denominator on the right hand side represents a spatial attenuation factor, obtained from a ratio of cross sections of energy flux at d and at the distance from the wave source to a point of interest $(y + d)$.

With regard to n in eq. (3), which expresses the degree of spatial spread of energy, let n in the xy plane be nxy and n in the yz plane be nyz, then n = nxy + nyz. Accordingly, n = nxy + nyz = 0 + 0 = 0 for the plane wave in the case where the point of observation is far from the antenna, n = nxy + nyz = 1 + 0 = 1 for the cylindrical wave when a line source is arranged parallel to the z axis, and n = nxy + nyz = 1 + 1 = 2 for the spherical wave radiated from a point source.

Furthermore, when energy spreads in a plane shown in Fig. 3(a), n(z) is constant at a point on the line parallel to z axis. When energy spreads circularly shown in Fig. 3(b), the value of n(θ) is constant on the arc of the circle, whose center is a point of a wave source.

4.1. LINE SOURCE CLOSE TO THE MEDIUM

As in the case where the half-wavelength dipole is close to the human head model, Fig. 4 shows the attenuation characteristic of the SAR when $d = 5$ mm. The ○ marks are calculated results using the FDTD. The Δ marks are experimental data achieved by the electric field probe method [7] under the same condition as in the analysis. It is found from Fig. 4 that the analytical values concurred precisely with the measured values, proving the effectiveness of the FDTD analysis.

In Fig. 4, each thin line is the attenuation characteristic when n = 0, 1, and 2 in eq. (3). The bold line represents the attenuation characteristic when n = 0.8 in eq. (3), obtained by best fitting the data calculated by the FDTD to eq. (3) using the least mean square method. Figure 4 indicates that attenuation characteristic obtained from eq. (3) of n = 0.8 is in good agreement with the calculated results. Since n is obtained to be about 1, it is considered that the energy spreads as a cylindrical wave in the medium.

Figure 5 shows the distribution of the SAR in the xy and yz planes calculated using the FDTD analysis when the half-wavelength dipole is close to the medium. The value of the SAR is normalized by the maximum value and shown in dB. In this case, the spread of energy is considered to be a cylindrical wave since the wave source is linear.

Figures 6(a) and (b) show n's as a function of φ in the xy plane and as a function of z in the yz plane, obtained from Fig. 5. In Fig. 6, we can see that both n(φ) and n(z) are constant. These phenomena indicate that the energy spreads circularly in the xy plane as emission from a point source and is kept to be constant in the yz plane because of a line source.

4.2. POINT SOURCE CLOSE TO THE MEDIUM

It was revealed that the spatial spread of energy in a lossy medium is like a plane wave when the source is far from the medium as shown in Fig. 2 and a cylindrical wave when close to the medium shown in Fig. 4. Based on this fact, it is estimated that the energy spreads with a spherical wave when the point source is located near the medium. Therefore, in order to examine this conjecture, the attenuation characteristic is investigated when a short dipole antenna is located near the medium.

Figure 7 shows the attenuation characteristic of the SAR when a short dipole antenna (λ/15 = 22 mm) is located at a distance d of 5 mm from the human head model. Figure 7 clearly shows that eq. (3) is a good approximation when n = 1.6. The energy spreads as a spherical wave because n is obtained to be about 2.

Figure 8 shows the distribution of the SAR calculated using the FDTD in the xy and yz planes when the dipole antenna with length of a λ/15 is close to the medium. From a comparison with Fig. 5(a) and Fig. 8(a), the distribution of the SAR of a short dipole is observed to be the same as that of the half-wavelength dipole since both the antennas function as a point source in the xy plane. On the other hand, in the yz plane, the distribution shown in Fig. 8(b) is found to be a little different from that shown in Fig. 5(b).

Figure 9(a) and (b) show n's as a function of φ in the xy plane and as a function of θ in the yz plane, obtained from Fig. 8. In Fig. 9, n(φ) in the xy plane and n (θ) in the yz plane are observed to be constant.

It can be stated from this consequence that the spread of energy is spherical since the antenna functions as a point source with regard to a wave in both the *xy* and *yz* planes.

5. CONCLUSION

The attenuation characteristic of the SAR in a lossy media was examined. As a result, it was revealed that when an antenna is placed close to a lossy media, the loss caused by the spatial spread of energy must be considered in addition to the loss due to the medium itself. Furthermore, the formula, which takes the spatial attenuation factor into consideration, is effective in estimating the attenuation characteristic of the SAR in the lossy medium.

REFERENCES

[1] N. Kuster and Q. Balzano, "Energy absorption mechanism by biological bodies in the near field of dipole antennas above 300 MHz," IEEE Trans. Veh. Tech., vol. 41, no. 1, pp. 17-23, Feb. 1992.

[2] N. Kuster, Q. Balzano, and J. Lin, Mobile Communications Safety, London, U. K. Chapman & Hall, 1997.

[3] R. Y-S. Tay, Q. Balzano and N. Kuster, "Dipole configurations with strongly improved radiation efficiency for hand-held transceivers," IEEE Trans. A. P, vol. 46, no. 6, pp. 798-806, Jun. 1998.

[4] William H. Hayt Jr. and John A. Buck, " Engineering Electromagnetics / six edition," McGraw-Hill, 2001.

[5] K. Ogawa, A. Ozaki, S. Kajiwara, A. Yamamoto, Y. Koyanagi, and Y. Saito, "High-Speed SAR Prediction for Mass Production Stages in a Factory by H-Field Measurements," to be published in IEEE AP-S Intl. Symp. Digest, June 2004.

[6] COST244 WG3, "Proposal for numerical canonical models in mobile communications, " Proc. of COST244, pp. 1-7, Roma, Nov. 1994.

[7] T.Schmid, O.Egger, and N. Kuster, "Automated E-field scanning system for dosimetric assessment," IEEE Trans. on MTT. 44, No.1, pp.105-133, Jan. 1996.
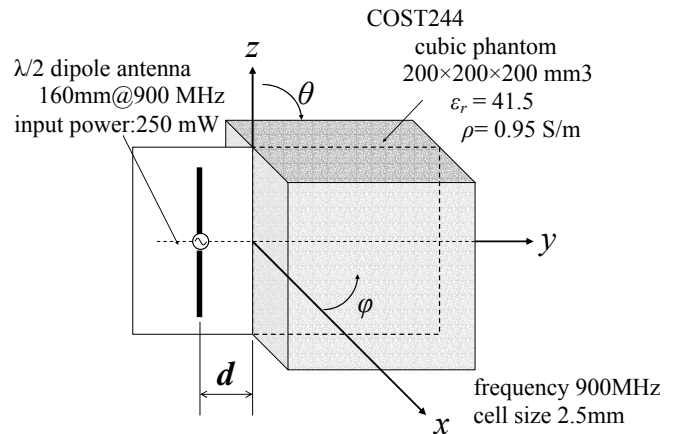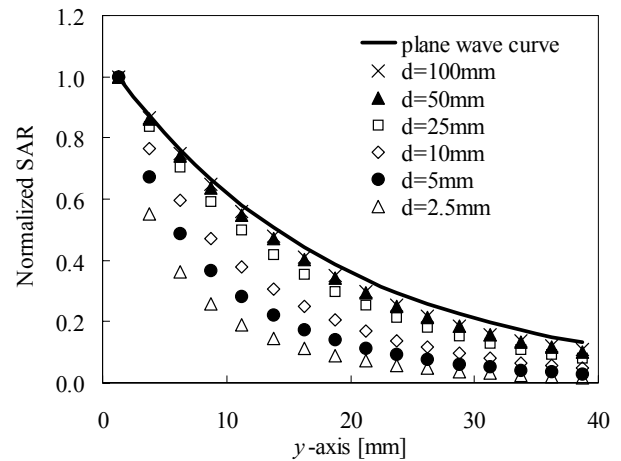
Fig. 1 : Calculation model.

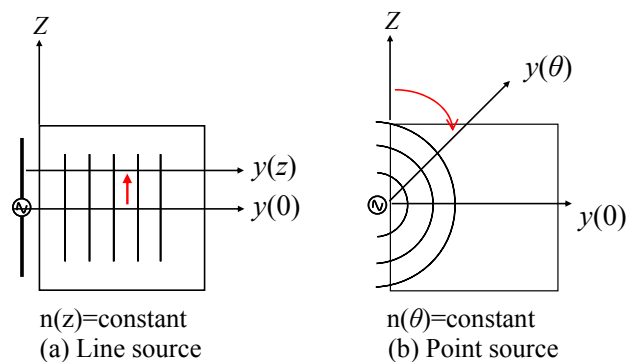Fig.2: Attenuation characteristics of SAR in a lossy media at 900MHz.

(a) Line source   (b) Point source
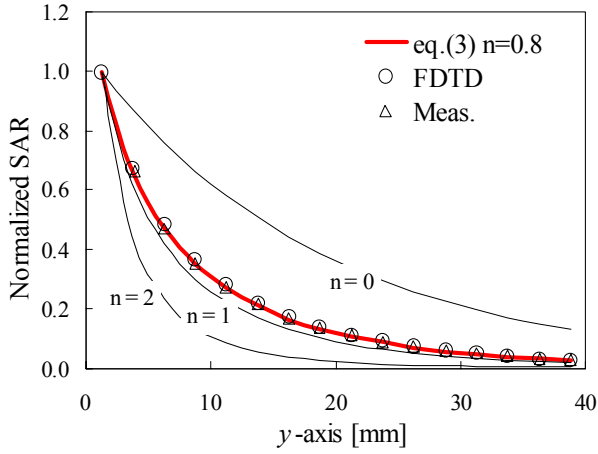
Fig.3: Extension of energy in a lossy media.

Fig.4: Attenuation characteristics of SAR in a lossy media with a λ/2 dipole antenna when *d* is 5mm.

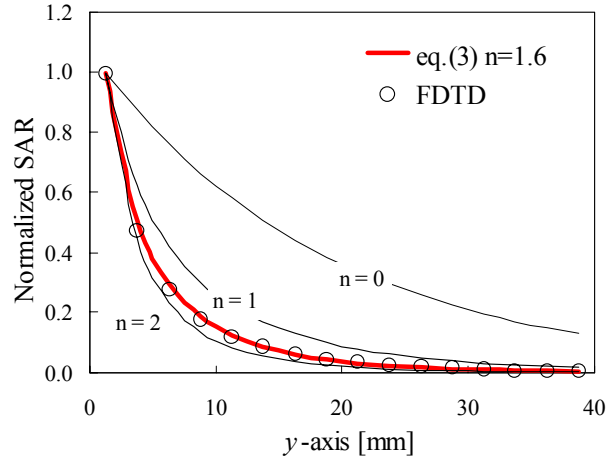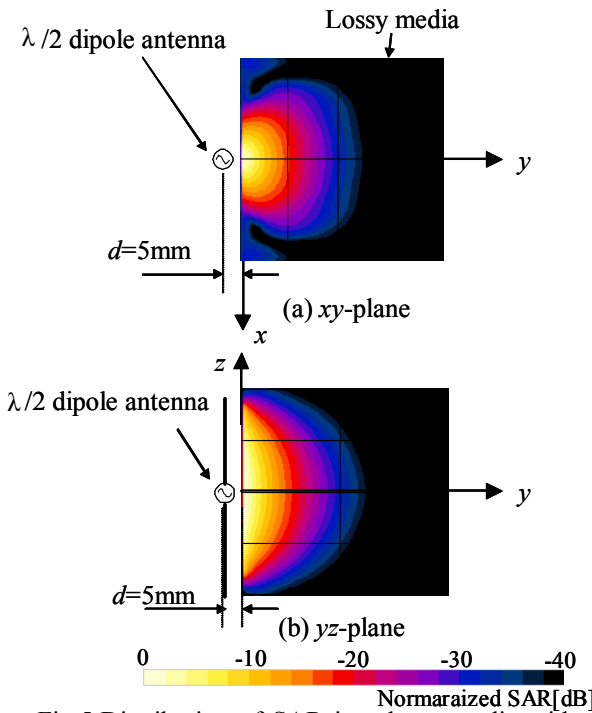Fig.7: Attenuation characteristics of SAR in a lossy media with a λ/15 dipole antenna when *d* is 5mm.

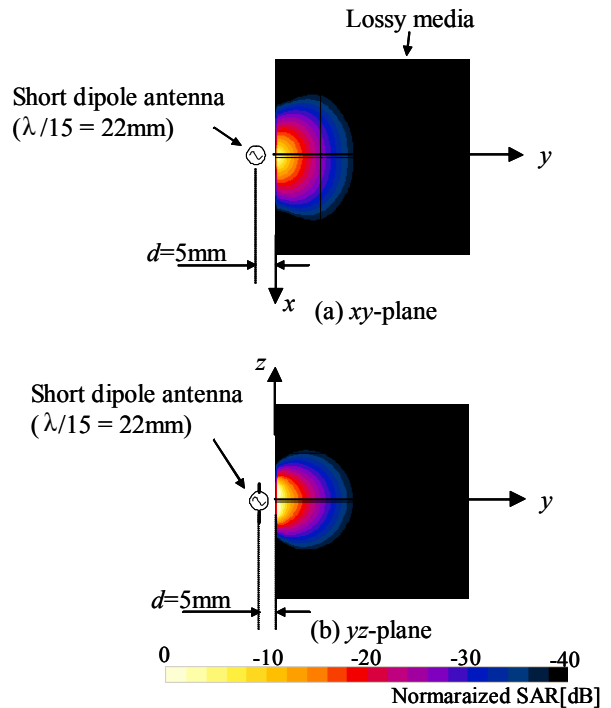Fig.5:Distribution of SAR in a lossy media with a λ/2 dipole antenna.

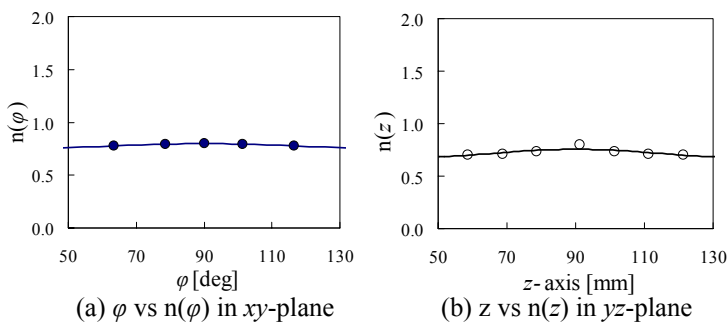Fig.8:Distribution of SAR in a lossy media with a λ/15 dipole antenna.

(a) *φ* vs n(*φ*) in *xy*-plane   (b) z vs n(z) in *yz*-plane

Fig.6 : n with a λ/2 dipole antenna when *d* is mm.
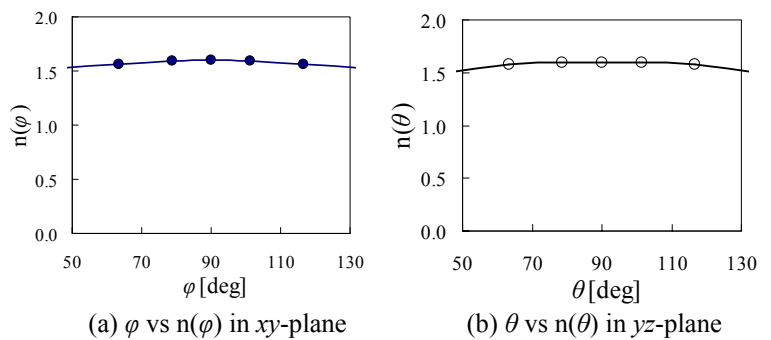

(a) *φ* vs n(*φ*) in *xy*-plane   (b) *θ* vs n(*θ*) in *yz*-plane

Fig.9 : n with a λ/2 dipole antenna when *d* is mm.